The Journal of Experimental Medicine

The Role of *Brg1*, a Catalytic Subunit of Mammalian Chromatin-remodeling Complexes, in T Cell Development

Thomas C. Gebuhr,[1] Grigoriy I. Kovalev,[2,4] Scott Bultman,[1] Virginia Godfrey,[3] Lishan Su,[2,4] and Terry Magnuson[1,4,5]

[1]*Department of Genetics,* [2]*Department of Microbiology and Immunology,* [3]*Department of Pathology and Laboratory Medicine,* [4]*Lineberger Comprehensive Cancer Center, and* [5]*Carolina Center for Genome Sciences, University of North Carolina at Chapel Hill, Chapel Hill, NC 27599*

Abstract

Mammalian SWI–SNF-related complexes use brahma-related gene 1 (*Brg1*) as a catalytic subunit to remodel nucleosomes and regulate transcription. Recent biochemical data has linked *Brg1* function to genes important for T lymphocyte differentiation. To investigate the role of SWI–SNF-related complexes in this lineage, we ablated *Brg1* function in T lymphocytes. T cell–specific *Brg1*-deficient mice showed profound thymic abnormalities, CD4 derepression at the double negative (DN; $CD4^-$ $CD8^-$) stage, and a developmental block at the DN to double positive ($CD4^+$ $CD8^+$) transition. 5′-bromo-2′-deoxyuridine incorporation and annexin V staining establish a role for Brg1 complexes in the regulation of thymocyte cell proliferation and survival. This *Brg1*-dependent cell survival is specific for developing thymocytes as indicated by the presence of *Brg1*-deficient mature T lymphocytes that have escaped the developmental block in the thymus. However, reductions in peripheral T cell populations lead to immunodeficiency and compromised health of mutant mice. These results highlight the importance of chromatin-remodeling complexes at different stages in the development of a mammalian cell lineage.

Key words: *Brg1* • SWI–SNF • chromatin • T cell • development

Introduction

Coordinated programs of gene expression underlie the development, functional differentiation, and homeostatic regulation of the mammalian immune system. Perhaps one of the most intensely studied systems of transcriptional regulation is that of T lymphocyte ontogeny (1). Activation or repression of lineage-specific and developmental stage–restricted cell surface molecules has been correlated with cell fate choices in the αβ T cell differentiation pathway. Up-regulation of both CD4 and CD8 and subsequent down-regulation of one of these two coreceptors in developing thymocytes leads to mature T helper ($CD4^+$ $CD8^-$) and cytotoxic ($CD4^-$ $CD8^+$) T cells in the periphery.

In addition to lineage-restricted transcription factors, it is becoming increasingly clear that chromatin-modifying factors are necessary to achieve proper temporal and spatial patterns of gene expression in the immune system. Modification of local chromatin structure is achieved, in part, through the activity of multisubunit protein complexes that use the energy of ATP hydrolysis to disrupt the conformation and position of nucleosomes (2). The yeast SWI–SNF complex was the first such complex to be identified. It has been characterized in the most detail and is conserved throughout evolution. Mammalian SWI–SNF-related complexes consist of 9–11 subunits that utilize either brahma (*Brm*; also called *SNF-α* or *Smarca2*) or *Brm*-related gene 1 (*Brg1*; also called *SNF2-β* or *Smarca4*) as the catalytic subunit (2, 3).

Targeted mutations of the *Brg1* catalytic subunit or two other complex members (*INI1–Snf5* and *Srg3–Baf155)* confer early embryonic lethality in the mouse, indicating that mammalian SWI–SNF-related complexes are essential (4–7). Although few direct target genes have been confirmed in mammalian cells, biochemical interactions with gene regulatory elements and transcription factors important for hematopoietic lineage specification have implicated SWI–SNF-related function in these processes (8). For example,

T.C. Gebuhr and G.I. Kovalev contributed equally to this work.

The online version of this article contains supplemental material.

Address correspondence to Terry Magnuson, Department of Genetics, Neurosciences Research Building, Room 4109D, University of North Carolina, CB 7264, 103 Mason Farm Road, Chapel Hill, NC 27599. Phone: (919) 843-6475; Fax: (919) 843-6365; email: trm4@med.unc.edu

Abbreviations used in this paper: BrdU, 5′-bromo-2′-deoxyuridine; *Brg1*, brahma-related gene 1; *Brm*, brahma; DN, double negative; DP, double positive; PI, propidium iodide; SP, single positive; TN, triple negative.

 J. Exp. Med. © The Rockefeller University Press • 0022-1007/2003/12/1937/13 $8.00
Volume 198, Number 12, December 15, 2003 1937–1949
http://www.jem.org/cgi/doi/10.1084/jem.20030714

interactions of chromatin-modifying complexes, including SWI–SNF-related, with *Ikaros*, a zinc finger–containing, sequence-specific DNA-binding transcription factor important in lymphocyte development, suggest a link between chromatin regulation and hematopoietic cell fate decisions (9). Consistent with this notion, chromatin immunoprecipitation assays have correlated down-regulation of IL-2Rα (CD25) at the double negative (DN) stages of T cell development with the dissociation of *Brg1* and histone acetylase p300 from promoter elements (10). Moreover, dominant negative expression of BAF57, an HMG-containing, DNA-binding subunit of the SWI–SNF-related complexes, in the T cell lineage revealed a role of chromatin remodeling in CD4 silencing and CD8 activation (11). These data provide evidence that SWI–SNF-related complexes are important regulators of stage-restricted gene expression in the T cell lineage. In addition to this developmental gene regulation, chromatin-modifying activity has been associated with proliferation of peripheral T lymphocytes. For example, antigenic activation of T cells induces rapid association of SWI–SNF-related complexes with chromatin in a *Brg1*-dependent manner (12). Furthermore, inactivation of Lsh, a member of the SNF2 family of proteins including *Brg1*, in lymphoid precursors results in a severe proliferation defect in response to Con A activation of peripheral T lymphocytes (13). Thus, chromatin-remodeling activity has been associated with a number of processes in T cell development and function, although the early lethality or minimal phenotypes associated with targeted mutations in SWI–SNF-related complex members do not permit loss of function studies in this lineage.

To investigate the in vivo role of Brg1 and the SWI–SNF-related complex function in T cell biology, we specifically inactivated *Brg1* in the T cell lineage using the Cre-*lox*P conditional mutagenesis system. Here, we report that loss of *Brg1* results in a block in T cell development at the immature stages and investigate the effect of *Brg1* mutation on mature T cells in the periphery. These data provide in vivo evidence implicating ATP-dependent chromatin-remodeling factors as important regulators of T lymphocyte development and immune response.

Materials and Methods

Mice. The *Brg1* germline-null allele (4), the *lck-Cre* (14), and the *Zp3-Cre* (15) mice have been described. The *Brg1* floxed allele mice were provided by P. Chambon (Centre National de la Recherche Scientifique, Strasbourg, France) and harbor previously described *lox*P sites integrated into the *Brg1* genomic locus (16). All mice were maintained on a mixed genetic background at the University of North Carolina, Chapel Hill Animal Facility.

Genotyping, RT-PCR, and PCR Quantification. Genotyping for the Brg1-targeted mutation has been described (4). For the detection of the *lck-Cre* and *Zp3-Cre* transgenes, similar conditions were used except for 1.5 mM $MgCl_2$, 62°C annealing temperature, and the following primers specific for Cre: forward, 5′caatttactgaccgtacac3′; reverse, 5′catcgccatcttccagcag3′. For the amplification of the unrecombined and recombined floxed allele depicted in Fig. 1 B the sequences are: primer 1, 5′-gatcagctcatgccctaagg-3′; primer 2, 5′-gtcatacttatgtcatagcc-3′; and primer 3, 5′-gccttgtctcaaactgataag-3′ (1 mM $MgCl_2$ and 51°C annealing). RT-PCR conditions for *Brm*, *TCRβ*, and CD3ε have been reported (4, 17, 18).

Quantification of PCR products was performed on a GelDoc 2000 (Bio-Rad Laboratories) using Multianalyst software (Bio-Rad Laboratories; see Supplemental Materials and Methods, available at http://www.jem.org/cgi/content/full/jem.20030714/DC1).

Antibodies, Cell Labeling, and FACS® Assays. mAbs used for immunofluorescence are listed in Supplemental Materials and Methods, available at http://www.jem.org/cgi/content/full/jem.20030714/DC1. Annexin-V/propidium iodide (PI) staining was performed according to the manufacturer's protocol (Roche). LN cells were stained and analyzed on a FACScan™ flow cytometer (BD Biosciences). Cell sorting was performed on a MoFlow (DakoCytomation) instrument. The FACS® data were analyzed with the Summit V3.1 data analysis software (DakoCytomation).

Histology. Thymi from 4-wk-old animals and livers from 3–6-mo-old animals were dissected, fixed in 4% paraformaldehyde, and processed for the production of paraffin sections. 5–8-μm sections were stained with hematoxylin and eosin using standard conditions.

In vivo 5′-bromo-2′-deoxyuridine (BrdU) Labeling and Anti-BrdU Staining. BrdU (Sigma-Aldrich) was administrated by intraperitoneal administration of 1 mg/mouse injected two times 4 h apart as previously described (19). Thymocytes were harvested in 1 h after the second injection and stained with anti-CD4 and anti-CD8 mAbs. The BrdU staining of those cells was performed by a conventionally modified method as previously described (19).

Cell Activation and Proliferation Assays. The complete medium (RPMI 1640 supplemented with 10% FCS, 2 mM L-glutamine, 50 U/ml pen/strep) was used for cell culture. CD3 and CD3/CD28 stimulation was performed as previously described (20). For in vitro mitogen stimulation, 5×10^5 LN cells were cultured in 200 μl medium, with or without 5 or 10 μg/ml Con A (Sigma-Aldrich), or with 0.5 ng/ml PMA and 0.5 μM ionomycin in 96-well flat-bottom plates. Incubation was performed in complete RPMI for 48 h in 37°C with pulse [H^3]thymidine at 1 uCi/well for the last 12 h.

Online Supplemental Material. See Supplemental Materials and Methods, available at http://www.jem.org/cgi/content/full/jem.20030714/DC1, for details regarding genotyping, RT-PCR, and PCR quantification.

Results

Generation of T Cell–specific Brg1-deficient Mice. To investigate the potential function of *Brg1* during thymocyte development, we used a previously described *Brg1* "floxed" allele in which *lox*P sites flank exons that encode a portion of the conserved ATPase domain (Fig. 1 A; references 4 and 16). Cre-mediated recombination of the *lox*P sites creates a deletion corresponding to the putative ATP hydrolysis site and also introduces a frameshift mutation. This "Δ floxed" configuration encodes a COOH terminally truncated protein product and is predicted to be a null allele, which was confirmed by crossing the floxed allele to a *Zp3-Cre* transgenic mouse that recombines *lox*P sites in the female germline (15). Constitutive Δ floxed/+ intercrosses failed to yield Δ floxed/Δ floxed homozygotes and no homozygotes were recovered upon dissection of litters

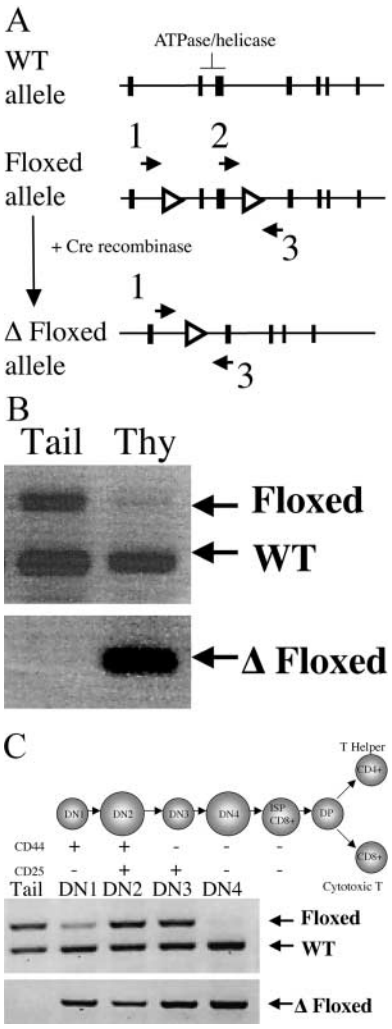

Figure 1. Conditional inactivation of *Brg1* in developing thymocytes. (A) Schematic representation of *Brg1* floxed allele. Open triangles represent position of *lox*P sites, solid boxes represent *Brg1* exons, and arrows 1–3 indicate position and orientation of PCR primers used for genotype analysis in C and D. (B) Detection of Cre-mediated deletion of the *Brg1* floxed allele in thymus. PCR analysis using primers (primer set 2/3 in B) that amplify both the wild-type and floxed allele (top) in whole thymus DNA preparations from +/floxed; *lck-Cre* mice. Loss of upper floxed allele band indicates efficient recombination of *loxP* sites and conversion to Δ floxed (bottom, primers set 1/3 in B). (C) Timing and efficiency of recombination during thymocyte development at the DN ($CD4^-$ $CD8^-$) stages. TN ($CD4^-$ $CD8^-$ $CD3^-$) thymocytes from +/floxed:*lck-Cre* mice were subdivided into DN1→DN4 stages. PCR analysis as described in B allowed for determination of timing of recombination (bottom) and efficiency of recombination (top) at these DN stages using tail DNA as a control.

at embryonic days 7.5 and 8.5 (0/15; $0.05 > P > 0.025$). The fact that no resorption moles or empty decidua were observed indicates that lethality occurs before decidualization is initiated as reported for the targeted null allele (4). Thus, Δ floxed is a null allele.

Mice carrying the *Brg1* floxed allele (+/flox) were mated with mice heterozygous for a *Brg1*-null mutation generated by gene targeting (+/null) and mice expressing Cre recombinase under the control of the *lck*-proximal promoter (+/+; *lck-Cre*) to obtain compound heterozygous mice harboring the lck-Cre transgene (null/floxed; *lck-Cre*, henceforth referred to as $tBrg1^{-/-}$ for T cell lineage–specific *Brg1* mutation; references 4 and 14). Mice harboring one floxed allele, one wild-type allele, and the *lck-Cre* transgene (+/floxed; *lck-Cre*) showed no differences from wild-type mice in total thymocyte number or cell type composition (unpublished data), consistent with previously published reports of no gross abnormalities in T cell development in mice heterozygous for the *Brg1*-null mutation (11). Therefore, both wild-type and +/floxed; *lck-Cre* mice were used as controls.

The *lck-Cre* transgene has previously been shown to express Cre specifically in the T cell lineage, with Cre-mediated recombination detected as early as the DN1 ($CD44^+$ $CD25^-$) stage and complete by the double positive (DP; $CD4^+$ $CD8^+$) stage (14). PCR analysis of whole thymic DNA preparations from *Brg1* +/floxed; *lck-Cre* mice showed efficient recombination of *lox*P sites, as judged by the loss of the floxed amplicon (Fig. 1 B, top) using primers that amplify both the wild-type and floxed allele (Fig. 1 A, primers 2 and 3). Accordingly, the Δ floxed allele showed significant amplification in thymus and not in tail DNA preparations using primers specific for the recombined floxed allele (Fig. 1 B, bottom, and A, primers 1 and 3). To investigate timing of recombination of the *Brg1* floxed allele, we analyzed the triple negative (TN; $CD4^-$ $CD8^-$ $CD3^-$) DN1 through DN4 cell populations from *Brg1* +/flox; *lck-Cre* mice. Cre-mediated deletion began at DN1 and proceeded through DN4 (Fig. 1 C, bottom) stage, consistent with previous reports using this lck-Cre transgene (14). As shown in Fig. 1 C, top, the floxed allele was only partially deleted at the DN1, DN2, and DN3 stages, but was virtually complete by the DN4 stage. Loss of the floxed allele amplicon at DN4 indicates high efficiency of recombination by this stage.

T Cell–specific Brg1 Inactivation Resulted in Abnormal Thymic Development and Runting. Gross dissection of $tBrg1^{-/-}$ mutant animals revealed severe thymic defects. The overall size of the mutant thymus was markedly reduced compared with the large, bi-lobed thymus observed in control littermates at 4 wk of age (compare A and B in Fig. 2). Thymocyte cell counts demonstrated a dramatic 20-fold reduction in total thymocytes present in the mutant thymus, indicating a T cell developmental defect ($1.3 \pm 0.7 \times 10^7$ in mutant vs. $27.3 \pm 8 \times 10^7$ in control 4-wk-old thymus; Fig. 2 D). In support of this finding, histological analysis revealed an almost complete loss of corticomedullary architecture in $tBrg^{-/-}$ mutant animals (compare E and F in Fig. 2) and enlarged cortical thymocytes containing irregular oval nuclei with more open chromatin, which is indicative of more immature thymocytes (Fig. 2 H). Additionally, higher magnification histological analysis revealed an increase in the number of mitotic figures as well as apoptotic bodies in the mutant thymus (compare G and H in Fig. 2).

$tBrg1^{-/-}$ mice displayed a significant reduction in body weights at 3–4 wk of age compared with sex-matched control littermates (Fig. 2 C). Although the severity of runting was variable between litters, differences in body weights

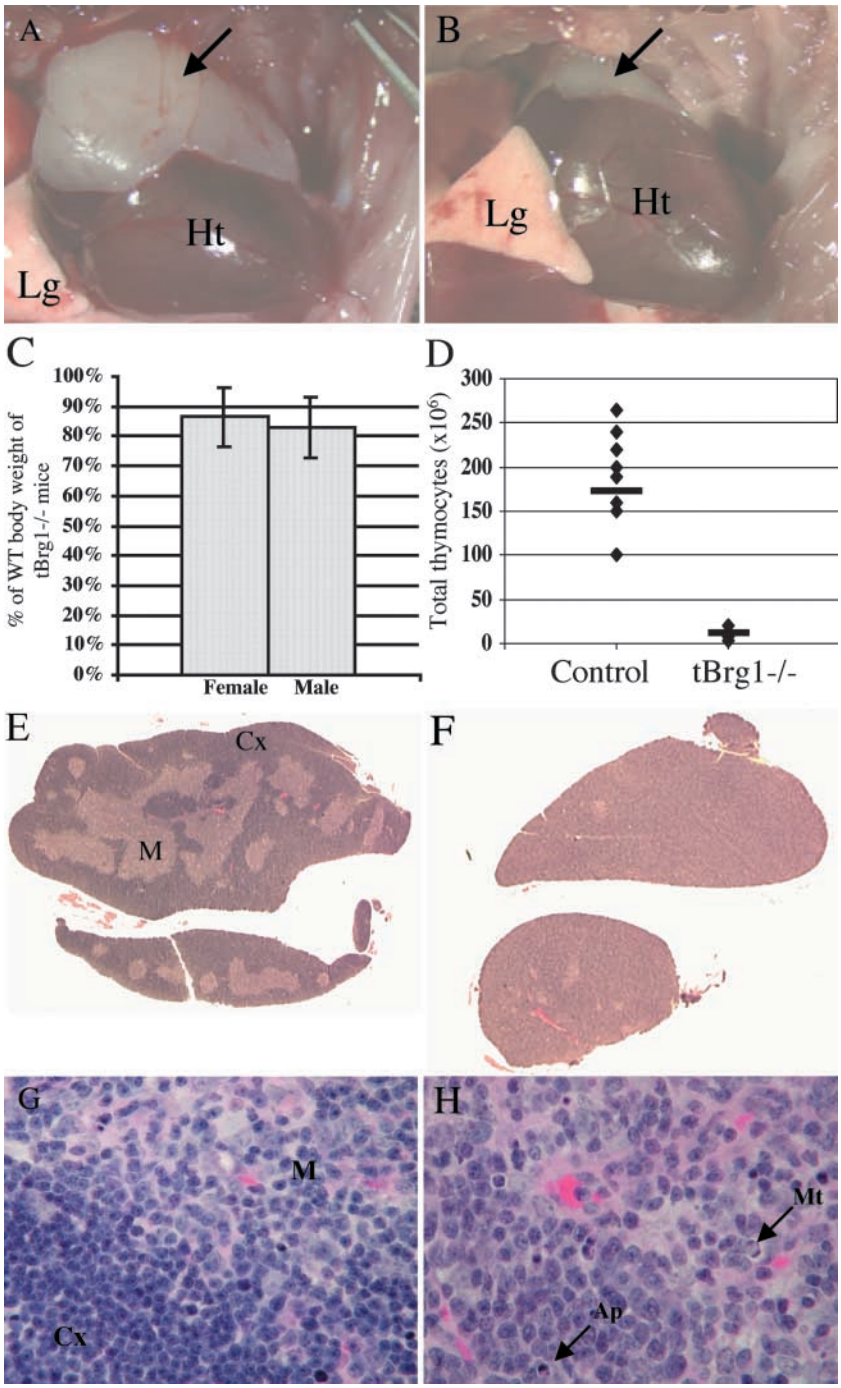

Figure 2. Thymic defects in tBrg1$^{-/-}$ mutant mice. (A and B) Gross morphology of control (A) versus tBrg1$^{-/-}$ mutant (B) thymi of 4-wk-old animals. Arrows indicate bi-lobed thymus above heart in upper thoracic cavity. Heart (Ht) and lung (Lg) tissue are indicated. (C) Bar graph representation of mutant body weights. Bars represent averages of tBrg1$^{-/-}$ weights at weaning from multiple litters (left: female, $n = 5$; right: male, $n = 6$) expressed as percent of wild-type body weight (littermate controls). (D) Total thymic cellularity ($\times 10^6$) in control versus tBrg1$^{-/-}$ mice. Solid bars represent average values of total cell counts from individual mice (◆). control, $n = 8$; mutant mice, $n = 8$. (E–H) Hematoxylin and eosin–stained sections of control (E and G) and mutant (F and H) thymus. (F) Demonstrates loss of cortico-medullary (M, medulla; Cx, cortex) architecture in the mutant thymus at low magnification ($\times 10$). (H) Arrows indicate increased apoptotic bodies (Ap) and mitotic figures (Mt) observed in tBrg1$^{-/-}$ thymus on higher magnification ($\times 40$).

between mutants and control animals remained relatively constant throughout the aging process.

T Cell Developmental Block and CD4 Derepression in tBrg1$^{-/-}$ Mice. To provide insight into the nature of the T cell developmental defect, FACS® analysis of a number of stage-specific cell surface markers was performed on thymocytes from tBrg1$^{-/-}$ animals versus controls. Significantly, CD4/CD8 staining revealed an almost complete loss of the DP (CD4$^+$ CD8$^+$) and CD8 single positive (SP; CD4$^-$ CD8$^+$) cell populations, with a corresponding relative increase in DN (CD4$^-$ CD8$^-$) T cells in the mutant thymus (Fig. 3, A and B). Interestingly, mutant thymocytes showed an increased percentage of CD4 SP cells, although the absolute number of CD4$^+$ CD8$^-$ cells was reduced (Fig. 3, B and C). In absolute numbers per thymus, DP thymocytes were reduced 250-fold, CD4 SP fourfold, and CD8 100-fold, whereas the total DN cell population was largely unaffected (Fig. 3 C). Recently, SWI–SNF-related complexes have been implicated in the coordinated transcriptional regulation of CD4 (repression) and CD8 (activation) in developing thymocytes (11). Therefore, we hypothesized that the CD4$^+$ SP cells present in the tBrg1$^{-/-}$

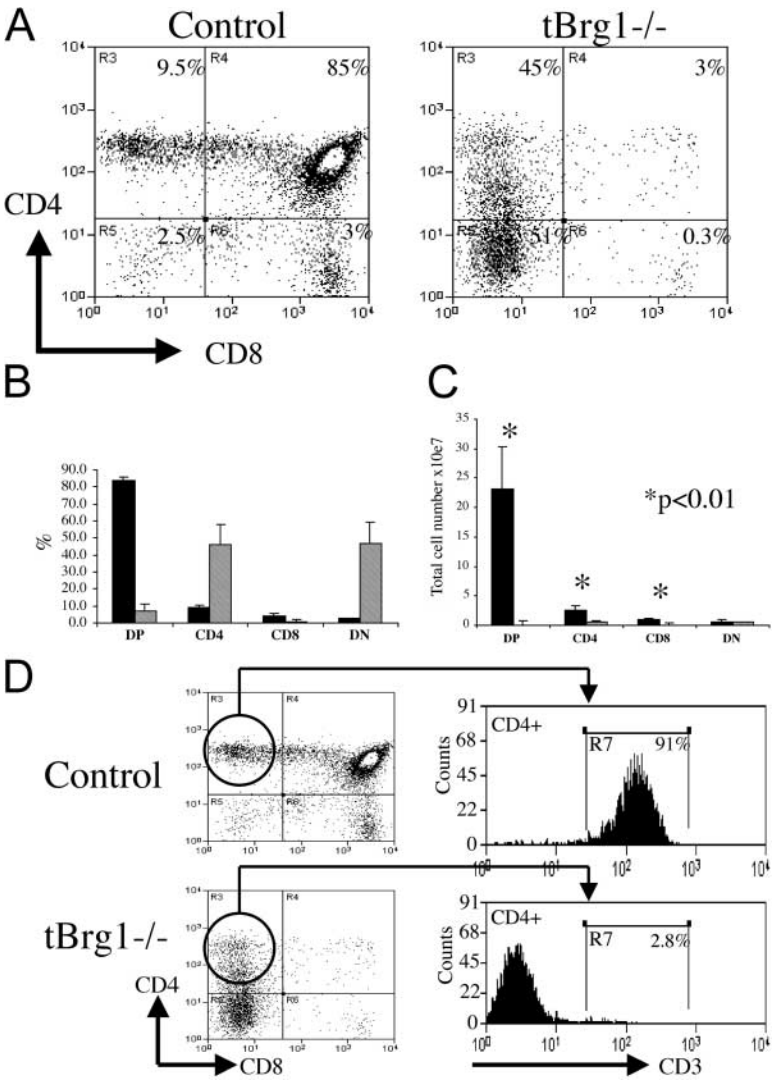

Figure 3. Block in T cell development at the DN stages in tBrg1$^{-/-}$ mice. (A) Flow cytometric analysis of CD4 versus CD8 expression on thymocytes from 4-wk-old tBrg1$^{-/-}$ mutant and control littermates. (B) Bar diagram showing average percentages for CD4$^+$ CD8$^+$ (DP), CD4 SP, CD8 SP, and CD4$^-$ CD8$^-$ (DN) subpopulations. Solid bars represent percentages from control mice (n = 9) and hatched bars represent tBrg1$^{-/-}$ thymic populations (n = 9). (C) Absolute cell numbers ($\times 10^7$/thymus) for thymocyte subsets described in B were calculated and are shown as bar diagrams. Solid bars (control) and hatched bars (tBrg1$^{-/-}$) represent average values. *, statistical significance calculated using the Student's t test (p-value indicated). (D) Analysis of TCR (CD3) surface levels in CD4$^+$ SP thymocytes in control (top) versus mutant (bottom). A low percentage of CD4 SP cells in tBrg1$^{-/-}$ mice express TCR compared with controls and therefore constitute immature T cells that have undergone CD4 derepression.

mutant thymus constitute an immature T cell population that aberrantly express CD4 (derepression) at the DN stages in the absence of *Brg1* function. Examination of TCR surface levels in mutant and control CD4$^+$ SP cells confirmed this hypothesis, with <5% of CD4$^+$ mutant thymocytes expressing high levels of the TCR compared with 90% TCR$^+$ observed in control mature CD4$^+$ SP cells (Fig. 3 D). Moreover, direct examination of CD4 expression at the DN stages demonstrated significant increases of CD4 levels in mutant thymocytes at DN2, DN3, and DN4 (Fig. 4, B and C). Finally, PCR analysis on mutant CD4$^-$ and CD4$^+$ DN3 thymocytes revealed a much higher percentage of mutant cells in the CD4$^+$ derepressed class than the CD4$^-$ cell population (see Fig. 6, bottom). Taken together, these data indicate that loss of *Brg1* function in developing thymocytes results in CD4 derepression and a block at the DN stages of T cell development.

To determine more precisely at which stage the developmental block occurred in the tBrg$^{-/-}$ mutant mice, DN thymocytes were subdivided into four distinct developmental stages (DN1, DN2, DN3, and DN4) based on cell surface expression of CD25 and CD44 expression on TN thymocytes (Figs. 4 A and 1 C). On a percentage basis, tBrg1$^{-/-}$ mice showed a relative increase in TN cells, as predicted by the loss of the DP population (see above), and this increased percentage translated into an increase in absolute terms as the total number of TN cells was significantly higher than in controls (Fig. 4 A). Examination of the DN1→DN4 populations from the mutant thymus revealed the total TN increase was attributed to increased DN2 and DN3 populations (Fig. 4 A), suggesting a developmental block and/or increased proliferation at these stages that should be reflected by decreased or increased DN4 population, respectively (Fig. 4 A). However, DN4 cell counts were similar in mutant compared with controls. This is most likely explained by CD4 derepression occurring in mutant thymocytes transitioning from DN2/DN3→DN4 stages (Fig. 4 B), which would exclude this population from DN4 cell counts. Given the almost complete deletion of the floxed allele at the DN4 stage, it is not clear why this population was not uniformly affected (CD4 derepression). In DN4 cells that have undergone

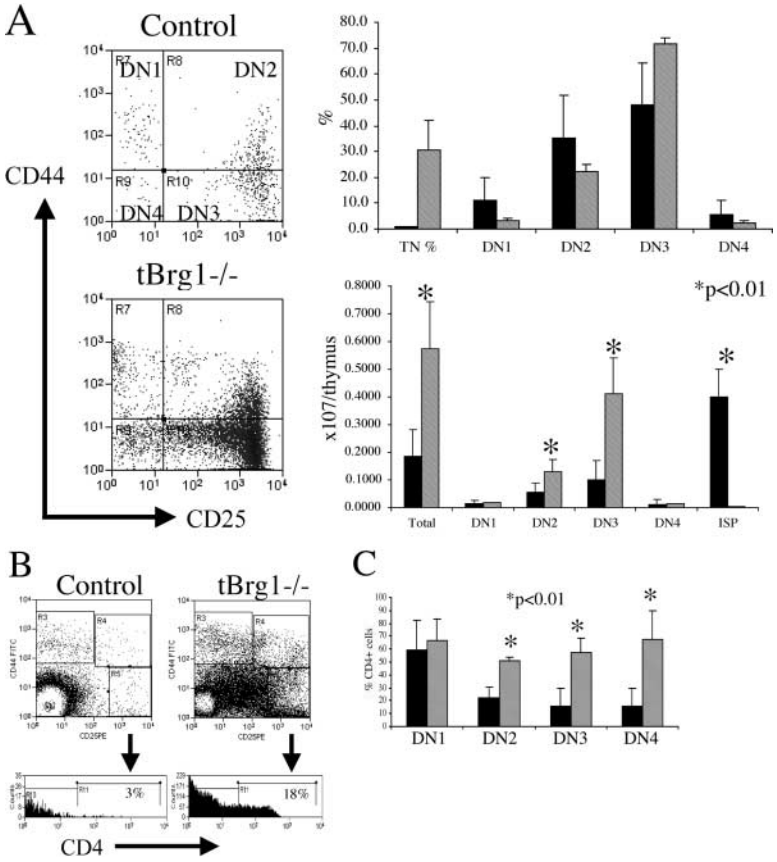

Figure 4. Loss of *Brg1* derepresses CD4 expression and induces arrest at the DN stages of thymocyte development. (A) Flow cytometric analysis of early thymocyte precursors in control (top) versus tBrg1$^{-/-}$ mutant (bottom). TN (CD4$^-$ CD8$^-$ CD3$^-$) cells were analyzed for expression of CD44 and CD25 (DN1 through DN4 stages, Fig. 1 C). Bar graph (top right) representing average percentages of the different subsets DN1, DN2, DN3, and DN4 in control (solid bars) versus mutant (hatched bars). Lower right bar graph represents absolute cell numbers ($\times 10^7$) for the subsets described in Fig. 1 C. tBrg1$^{-/-}$ mice are represented by hatched bars ($n = 3$) and control population are represented by solid bars ($n = 3$). (B) Flow sorting scheme to investigate CD4 expression at DN stages in control (left) versus tBrg1$^{-/-}$ mutant (right). TCR$^{-/low}$ cells were subdivided into DN1→DN4 (Fig. 1 C, top) and then analyzed for CD4 expression at the DN3 stage (bottom; reference 11). (C) Bar graph representing percentage of DN (DN1→DN4) cells that express CD4. Solid bars represent average value from controls ($n = 3$) and hatched bars represent average value from tBrg1$^{-/-}$ mutant ($n = 3$). *, p-value (Student's *t* test).

Cre-mediated recombination but do not express CD4, it is likely that residual Brg1 protein–loaded prior loss of the floxed allele is sufficient to repress CD4 expression at this stage. Regardless, the remaining DN4 cells were blocked in differentiation based on the absence of DP cells. In support of a DN4 to DP block, immature CD8 SP cells, the immediate precursors of the DP stage, are severely reduced in the mutant thymus (Fig. 4 A). Complicating this interpretation, however, is data implicating the SWI–SNF complex in direct regulation of CD8 expression (11). Therefore, it is unclear whether the reductions in cell numbers at the immature SP stage are due to block before this stage or fail to activate CD8 expression. Taken together, these data are consistent with developmental abnormalities beginning at the DN2/DN3 stage and subsequently with a block at the DN4→DP transition in tBrg1$^{-/-}$ thymocytes.

Increased Cell Proliferation and Apoptosis in tBrg1$^{-/-}$ Immature Thymocytes. To further investigate the increases in DN2/DN3 populations and determine the fate of the CD4$^+$ CD3$^-$ thymocytes, the proliferative status of mutant thymocytes was measured through in vivo BrdU incorporation. In tBrg1$^{-/-}$ mice, BrdU incorporation was significantly higher in both the DN and CD4 derepressed immature cell populations compared with controls (Fig. 5 A). Additionally, a slightly higher percentage of DP cells stained positive for BrdU$^+$, however the low numbers of DP cells present in the mutant thymus make this data unreliable. To characterize the proliferative status at the immature stages, DN cell populations were divided into two subclasses based on CD44 expression: CD44$^+$ (DN1+2) and CD44$^-$ (DN3+4). Interestingly, both subclasses showed an increased percentage of BrdU$^+$ cells in the mutant thymus (Fig. 5 B), indicating increased cell proliferation throughout the DN stages. This result is consistent with the histological observation of increased mitotic figures in the mutant thymus and increased total cell numbers at DN2 and DN3 in mutant mice (Figs. 2 H and 4 A).

Although the increased proliferation observed in the tBrg1$^{-/-}$ mice is consistent with an increase in total TN cells (Fig. 4 A), the severe reduction in total thymocytes present in mutant thymus cannot be fully explained by the inability of cells to proliferate. Therefore, we used the annexin V staining method to assay the percentage of cells undergoing apoptosis (21). Analysis of annexin V staining revealed a slight increase in the percentage of apoptotic DN thymocytes in mutant compared with controls (Fig. 5 C). Although these differences are unlikely to account for the massive cell loss in the mutant thymus, examination of annexin V staining in the mutant CD4 derepressed class (CD4$^+$ CD8$^-$ CD3$^-$) did demonstrate high percentages of cells undergoing apoptosis (Fig. 5 C; $P < 0.01$). These data are consistent with increased numbers of apoptotic bodies observed through histological analysis (Fig. 2 H). Taken together, these data suggest that loss of *Brg1* triggers an increase in cell proliferation, derepression of CD4, and sub-

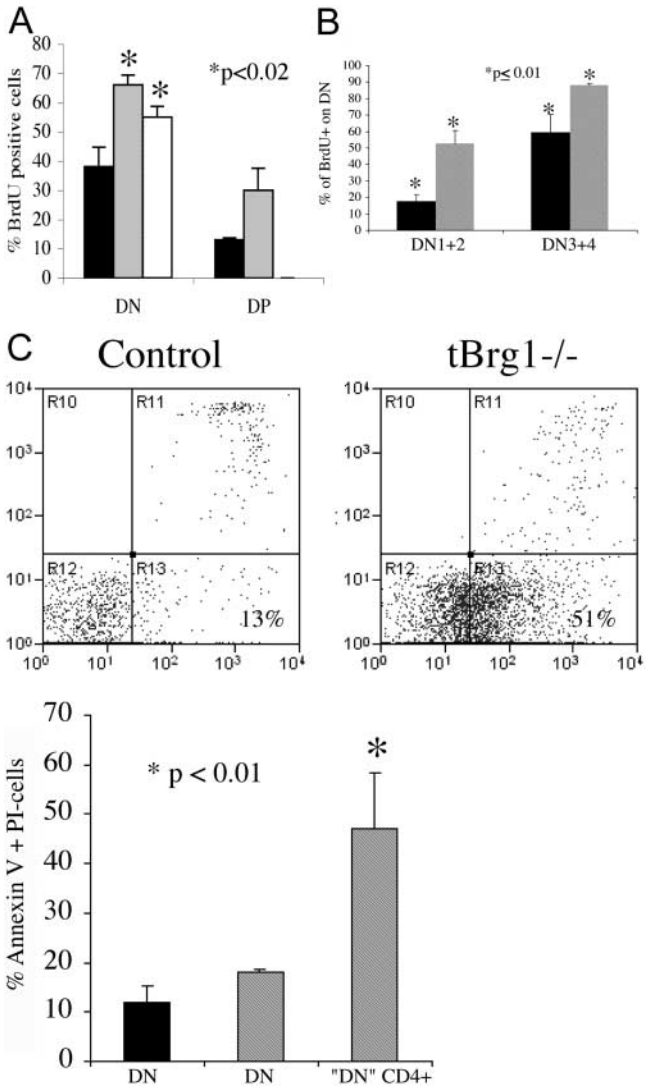

Figure 5. Cell proliferation and cell death at immature stages of T cell development in tBrg1$^{-/-}$ mice. (A) Bar graph representing average percentages of cells staining positive for BrdU incorporation on FACS®. Immature stages represent control DN (solid bar, $n = 3$), mutant DN (gray bar, $n = 3$), and mutant CD4 derepressed subpopulation (CD4$^+$ CD8$^-$ CD3$^-$, open bar, $n = 3$). *, statistical significance using Student's t test (p-value indicated). (B) Average percentage of BrdU incorporation at the DN1/DN2 and DN3/DN4 stages in control (solid bar) versus mutant (hatched bar). (C) Annexin V/PI staining of apoptotic cells on CD4$^+$ cells from mutant versus control (top). Bar graph representation (bottom) of percentage of cell staining positive for annexin V/PI$^-$. Solid bar indicates percentage of cells from control DN (CD4$^-$ CD8$^-$, $n = 3$). Hatched bars indicate percentage of apoptotic cells from tBrg1$^{-/-}$ mutant in total DN and CD4 derepressed class (CD4$^+$ CD8$^-$ CD3$^-$, $n = 3$).

sequently, programmed cell death at the DN stages of T cell development.

Brm and pre-TCR Expression Are Independent of Brg1. Based on the timing and severity of defects in *Brg1*-deficient thymocyte development, we investigated potential molecular abnormalities associated with the observed thymic phenotype. Specifically, we examined whether the loss of *Brg1* affected the expression of *Brm*, another SWI–SNF-related catalytic subunit often coordinately down-regulated in human tumor cell lines (22). As shown in Fig. 6, CD4$^+$ derepressed DN3 thymocytes exhibit efficient recombination of the floxed allele, indicating high proportion of mutant cells, but similar levels of *Brm* expression through semiquantitative RT-PCR analysis, indicating that *Brm* expression is independent of *Brg1* and does not contribute to the severity of the thymic phenotype. Additionally, we examined the expression of two components of the pre-TCR complex (TCRβ and CD3ε), which, when mutated, block thymocyte development at the DN3→DN4 transition (23). Both TCRβ and CD3ε were expressed at similar levels in mutant and control DN3 thymocytes (Fig. 6), suggesting that *Brg1* deletion impairs thymocyte developmental processes downstream of pre-TCR assembly.

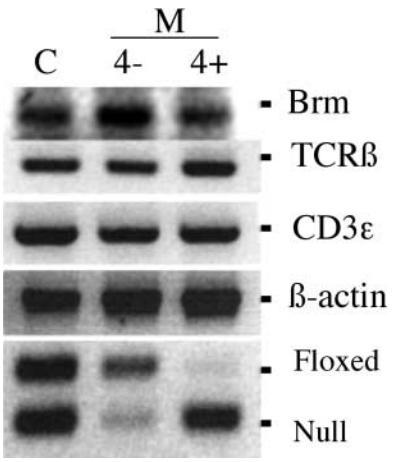

Figure 6. Expression analysis of Brg and TCR at the DN3 stage. RT-PCR measuring Brm, TCRβ, and CD3ε expression in control (C), mutant (M), CD4$^-$ (4−), and CD4$^+$ (4+) DN3 cells. β actin was used as a control for loading. The bottom represents PCR analysis (described in Fig. 1 B) to analyze Cre-mediated deletion of the floxed allele in the DN3 cell populations.

Cell Populations in the Periphery of tBrg1$^{-/-}$ Mice. To assess the degree of developmental block in the thymus and to determine whether Brg1 function is required for the survival of mature T cells, we used FACS® on LN and spleen cells to examine peripheral T cell populations in tBrg1$^{-/-}$ mice. Surprisingly, CD4/CD8 staining of peripheral lymphocytes indicated mature CD4$^+$ and CD8$^+$ cells present in the periphery of the mutant animals, although at significantly reduced levels, suggesting an incomplete developmental block in the thymus and/or failure of Cre-mediated recombination in a low percentage of "escaping" cells. To address this issue, we performed PCR amplification for the presence of the deleted floxed allele in whole LN preparations from mutant animals. Results from this analysis demonstrated that *Brg1* mutant cells were present in the LN, suggesting that the peripheral T cells were not exclusively cells that had escaped Cre-mediated recombination (Fig. 7 G).

Although total LN cell counts were similar in mutant compared with control (Fig. 7 A), TCR$^+$ cells were reduced fourfold in mutant mice with both the CD4$^+$ and

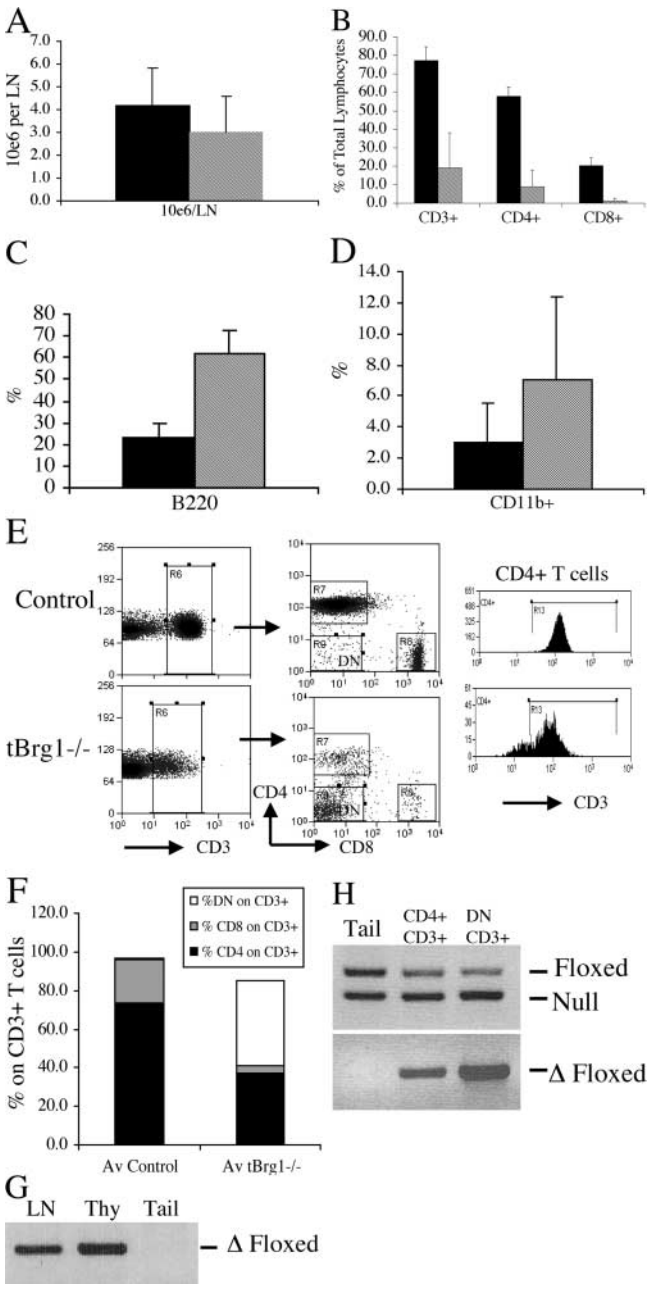

Figure 7. Peripheral T cell populations in tBrg1$^{-/-}$ mice. (A) Total LN cell counts represented in bar graph format for control (solid bars, $n = 9$) and mutant (hatched bars, $n = 11$). (B) Bar graph representation of percentages of CD3$^+$, CD4$^+$, and CD8$^+$ cells in control (solid bars, $n = 9$) and mutant (hatched bars, $n = 11$) LN. (C and D) Percentages of B cells (B220$^+$, C), and myeloid (CD11b$^+$, D) are represented in bar graph format for control (solid bars, $n = 9$) and mutant (hatched bars, $n = 11$). (E) Flow sorting analysis for CD4 and CD8 expression on CD3$^+$ lymphocytes (left and middle) revealing increased DN (CD4$^-$ CD8$^-$ CD3$^+$) cell populations in mutant LNs (middle). Histogram comparing TCR (CD3) surface levels on mutant and control CD4$^+$ cells (right). (F) Average percentage of CD4$^+$, CD8$^+$, and CD4$^-$ CD8$^-$ (DN) on CD3$^+$ T cells. Increased DN percentages in mutant mice are represented by open bar. CD4$^+$ CD3$^+$ (solid) and CD8$^+$ CD3$^+$ (hatched) percentages are shown for mutant (tBrg1$^{-/-}$, $n = 11$) and control ($n = 9$). (G and H) Presence of *Brg1* mutant lymphocytes in the periphery. In G, whole LN DNA preparations from mutant animals were tested for amplification of the Δ floxed allele (primer set 1/3). Thymus (Thy) served as a positive control and tail DNA as a negative control. PCR analysis of flow-sorted CD4$^+$ (CD4$^+$ CD8$^-$ CD3$^-$) and CD4$^-$ (CD4$^-$ CD8$^-$ CD3$^-$) populations from tBrg1$^{-/-}$ animals (H) indicated a mixture of mutant cells (bottom) and unrecombined floxed (top) cells in each population.

CD8$^+$ populations significantly underrepresented (sevenfold and 20-fold, respectively; Fig. 7 B). Increased numbers of B cells and myeloid cells compensate for the reduced numbers of T cells in the mutant LN and account for the equivalent total LN cellularity observed (Fig. 7, C and D). Interestingly, analysis of CD4 and CD8 expression on CD3$^+$ cells revealed a significant increase in DN TCR$^+$ cells (CD4$^-$ CD8$^-$ CD3$^+$; Fig. 7 E, middle, and F). This result could potentially be explained by increased percentages of γδ-TCR (CD4$^-$ CD8$^-$) T cells due to loss of αβ-TCR T cells in the periphery. However, calculation of total DN CD3$^+$ T cells indicated an increase in absolute number of this cell type in tBrg1$^{-/-}$ compared with controls ($1.5 \pm 0.2 \times 10^5$ vs. $0.6 \pm 0.1 \times 10^5$; $P < 0.01$). FACS® analysis for γδ-TCR cells in LN populations revealed that 80 ± 9.4% of mutant DN CD3$^+$ cells are γδ-TCR$^+$ compared with 28.7 ± 3% in controls. Similarly, absolute numbers of γδ-TCR T cells were increased in mutants ($1.2 \pm 0.12 \times 10^5$ in mutant vs. $0.18 \pm 0.05 \times 10^5$ in controls; $P < 0.01$). This result was surprising given that the size of the γδ-TCR T cell population has been shown to be regulated independently of the αβ-TCR T cell population (24). Additionally, significantly higher numbers of CD4$^+$ T cells stained positive for γδ-TCR in mutant compared with controls (20.1% or $0.15 \pm 0.03 \times 10^5$ vs. 0.05% or 0.07 ± 0.010^5 in controls; $P < 0.05$) and likely represent γδ-TCR T cells that have undergone CD4 derepression (see above). The *lck* proximal promoter has been shown to be active at the DN1 stage before αβ/γδ lineage commitment (Fig. 1 C; reference 25) and raised the possibility that *Brg1* inactivation in these early stages of T cell development influenced αβ/γδ cell fate decisions in the thymus. Arguing against this interpretation, absolute numbers of γδ-TCR$^+$ cells were not significantly increased in the mutant thymus ($1.45 \pm 0.6 \times 10^6$ in mutant vs. $1.04 \pm 0.3 \times 10^6$ in control) and suggested the increase in γδ-TCR$^+$ cells in mutants is due to peripheral expansion of this population. If this expansion in γδ-TCR cells were a direct result of loss of *Brg1* function, a prediction would be high percentages of *Brg1* mutant cells in this cell type. Therefore, we performed PCR analysis on CD4$^+$ CD8$^-$ CD3$^+$ and DN CD3$^+$ flow-sorted populations to test whether mutant cells contributed exclusively to the DN CD3$^+$ population. This prediction was not borne out experimentally, however, because both the CD4$^+$ SP and the DN populations amplified with primers specific for the recombined floxed allele (Fig. 7 H), indicating mutant cell contribution to both cell types. To examine relative contribution of mutant cells to these cell populations, we amplified the unrecombined floxed allele and null alleles (the targeted null mutation and the wild-type allele amplify the same 230-bp fragment, which is different from the 387-bp

fragment for the Δ floxed allele). Comparison of unrecombined floxed versus wild-type band intensity allowed us to estimate the percentage of undeleted floxed allele lost due to Cre-mediated conversion to Δ flox. We determined ~25% of the $CD4^+$ $CD8^-$ $CD3^+$ cells and 40% of the DN $CD3^+$ population were mutant for *Brg1*. Given that 20% of $CD4^+$ $CD8^-$ $CD3^+$ and 80% of DN $CD3^+$ cells are γδ-TCR^+, it raises the possibility that most of the *Brg1* mutant cells are γδ-TCR cells. In this scenario, loss of *Brg1* might be less detrimental to γδ-TCR cells and therefore allows for survival of this cell type. However, the inability to separate mutant (undergone Cre-mediated recombination) and heterozygous (escaped Cre-mediated recombination) T cells precludes direct examination of TCR or CD4/CD8 expression on mutant T cells. Although, significantly, these results suggest that, at least in the mature T cell lineage, Brg1 is not a general cell survival factor. In addition, loss of *Brg1* function in this lineage does not lead to increased incidence of cancer due to the absence of T cell neoplasia (leukemia and/or lymphomas) in a cohort of mutants aged over 18 mo.

Functional Characteristics of T Lymphocytes from tBrg1$^{-/-}$ Mutant Mice. Taking advantage of this "mosaic" (with respect to *Brg1* functional status) population of T cells, we sought to investigate potential T cell functional abnormalities, either cell autonomous or noncell autonomous, attributed to *Brg1* mutation. FACS® analysis of $CD4^+$ T lymphocytes from tBrg1$^{-/-}$ mutant mice revealed reduced surface levels of the TCR (Fig. 7 E), which has been implicated as a hallmark of TCR-mediated activation of T cells (26). Moreover, expression levels of CD44 and CD69, markers that are up-regulated upon naive T cell activation, were found to be increased on these T cells (Fig. 8 A). In addition to marking activated T cells, CD44 up-regulation has been shown to persist into the memory pool (27). Therefore, the dramatic up-regulation observed in tBrg1$^{-/-}$

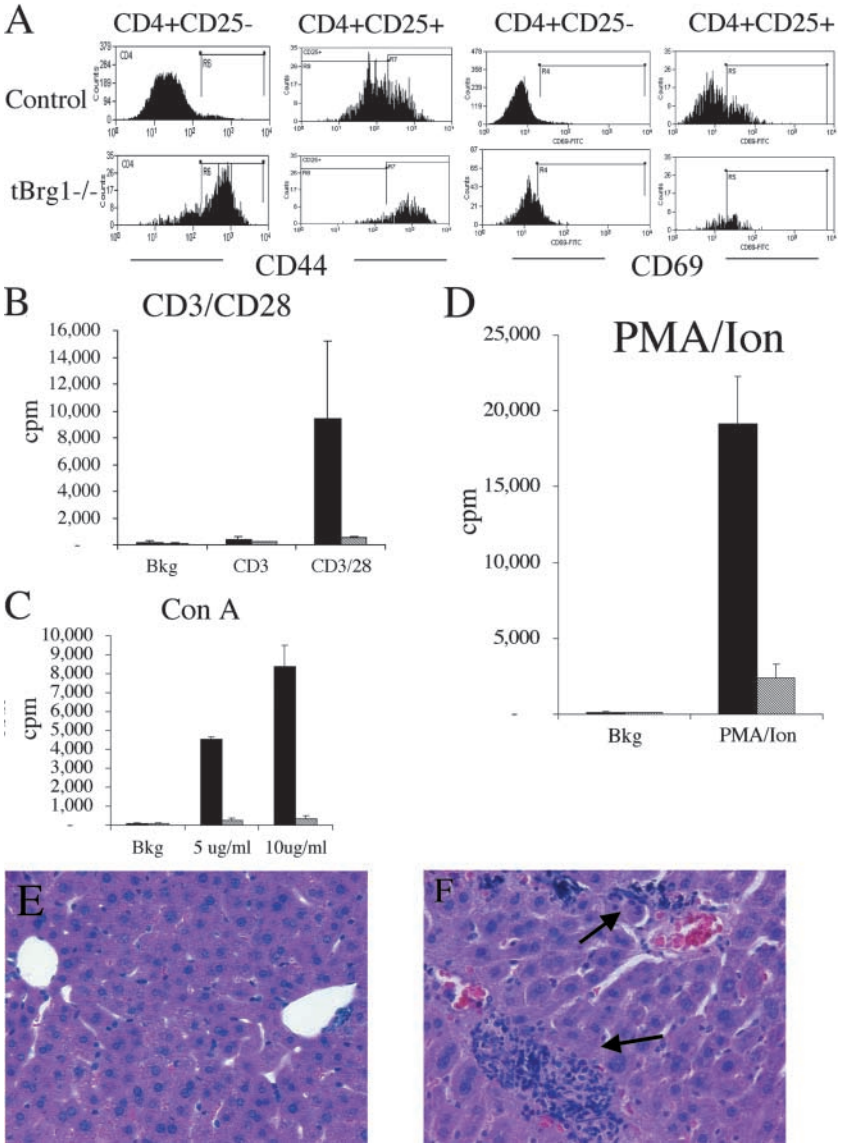

Figure 8. Functional characteristics of T lymphocytes from tBrg1$^{-/-}$ mice. (A) FACS® analysis of CD44 and CD69 on mutant and control $CD4^+$ lymphocytes. (B–D) Proliferative response of whole LN preparation from mutant (hatched bars) and control (solid bars) LNs using CD3/CD28 antibodies (B), Con A (C), and PMA/Ion (D) stimulation. (E and F) Hematoxylin and eosin–stained liver sections from 6-mo-old control (E) and mutant (F) littermates. Arrows indicate regions of periportal lymphocyte infiltration.

peripheral T cells (>70% of cells $CD44^+$ in mutant vs. <10% $CD4^+$ $CD44^+$ in controls) indicates that these cells are effector cells or that they have undergone prior activation and are memory-like T cells. To distinguish between these possibilities, we used IL-2Rα (CD25), another marker shown to be expressed on activated T cells, in concert with CD44 and CD69, an early marker of activation. Triple staining experiments indicated a moderate increase in $CD4^+$ $CD25^+$ $CD44^+$ (78.7 ± 2.1% in mutant vs. 32.8 ± 2.5% in controls) and $CD4^+$ $CD25^+$ $CD69^+$ (45.0 ± 9.0% in mutant vs. 31.5 ± 6.0% in controls) cells in mutant mice (Fig. 8 A). Collectively, these data demonstrate that mature T cells in the periphery of $tBrg1^{-/-}$ mice display features indicative of conversion of naive T cells to activated and/or memory-like state. Similar memory-like T cell phenotypes are characteristic of naive T cells that proliferate (called homeostatic proliferation) in response to conditions of lymphopenia after adoptive transfer into sublethally irradiated or genetically modified T cell–deficient hosts (28). The severe block in thymocyte development and the low numbers of DP cells in the $tBrg1^{-/-}$ mice suggests that the lymphopenic environment created by *Brg1* mutation in the mouse induces homeostatic proliferation of peripheral T cells.

To examine the functional consequences of loss of *Brg1* function in peripheral mature T cells, we determined in vitro proliferative responses to a number of stimuli including TCR cross-linking using anti-CD3 or anti-CD3 plus anti-CD28, Con A, and PMA/Ion. Activation of total LN cells from $tBrg1^{-/-}$ showed a significant reduction in T cell proliferative response for CD3 alone or CD3/CD28, two different concentrations of Con A, and PMA/Ion stimulation when compared with controls (Fig. 8, B–D). Significantly, these results indicate that $tBrg1^{-/-}$ mutant LNs cannot mount a significant T cell response and therefore can be classified as immunodeficient mice. Taken together, these results indicate that in $tBrg1^{-/-}$ mice, a small number of mutant and unrecombined heterozygous T cells escape the developmental block in the thymus and undergo limited homeostatic proliferation in the periphery that converts them to activated/memory-like T cells. These populations of T cells do not, however, completely fill the periphery, which results in immunodeficiency.

Aging of $tBrg1^{-/-}$ Mice Revealed Low Penetrance Lethality and Rectal Prolapse. The biological consequence, in terms of overall animal health, attributed to *Brg1* mutation in the T cell lineage was manifest at weaning (runting; Fig. 2 C) and throughout subsequent aging over a 12-mo period. Aging of mutant animals revealed low penetrance lethality. Roughly 15% of mutant animals (7 out of 49) died prematurely over a 12-mo period, whereas no lethality was observed in littermate control (+/floxed; *lck-Cre* and wild-type) animals (0 out of 72) over the same period. Furthermore, >20% (11 out of 49 in mutant vs. 0 out of 72 in controls) of mutant animals exhibited rectal prolapse over this aging period, although there was no correlation between the prolapsed rectums and premature lethality phenotypes. Based on the immunodeficiency observed in $tBrg1^{-/-}$ mice, these whole animal phenotypes were unexpected, as other immunologically compromised mice, such as RAG-deficient and nude mice, thrive in specific pathogen-free facilities similar to the one housing $tBrg1^{-/-}$ mice. Recently, it has been reported that infection of SCID/Ncr and nude mice with *Helicobacter* (*Helicobacter hepaticus* and *Helicobacter bilis*) results in large bowel disease clinically detected by rectal prolapse (29, 30) and, in the case of *H. hepaticus*, mild periportal lymphocyte infiltration of the liver (31). Therefore, we sought to investigate whether endogenous *Helicobacter* infection was the causative agent of illness in $tBrg1^{-/-}$ mice. Indeed, fecal samples from our colony tested positive for both *H. hepaticus* and *H. bilis* using PCR analysis specific for these pathogenic bacteria (unpublished data). Moreover, hematoxylin and eosin–stained sections of mutant liver revealed mild to moderate periportal lymphocyte (mixed lineage) infiltration in $tBrg1^{-/-}$ mice and not in controls (compare G and H in Fig. 8). These results suggest that endogenous *Helicobacter* infections contribute to the health problems in immunodeficiency associated with *Brg1* mutation in the T cell lineage.

Discussion

Considerable interest in ATP-dependent chromatin-remodeling complexes has focused on delineating biochemical interactions and molecular mechanisms functioning at promoters to influence transcriptional regulation. These studies do not, however, address the function of these complexes in vivo and significantly less is known about the function of these complexes in the context of global gene regulation. The peri-implantation lethality observed in *Brg1* homozygous mutant mice demonstrated the importance of these complexes in early development but precluded further functional studies in cell lineages later in embryogenesis or adults. Here, we provide further insight into the function of Brg1 in an adult cell lineage by showing that the Brg1 complex is required for T cell development at the DN→DP transition but not for cell survival of mature T lymphocytes.

In $tBrg1^{-/-}$ mice, abnormalities in thymocyte differentiation are first manifest by an increased number of cells at the DN2/DN3 stage and subsequently by a block in development at the DN4→DP transition. This transition from DN3→DN4→DP is characterized by β selection checkpoints, the importance of which is underscored by mutations in genes involved in these processes. For example, mutations in the genes involved in TCRβ rearrangement (*Rag1* and *Rag2*), assembly of the pre-TCR (*TCRβ*, *pTα*, or *CD3ε*), or mediation of the signal transduction cascade from the pre-TCR ($p56^{lck}$/$p59^{fyn}$, Syk/ZAP70, or *SLP-76*) results in a block in development at the DN3 stage (23). Therefore, based on the phenotypic similarities between these mutants and $tBrg1^{-/-}$ mice, it is possible that the Brg1 complex(s) plays a role in the β selection process. In support of this notion, the human SWI–SNF complex was

shown to stimulate the cleavage and processing of DNA by RAG1 and RAG2 in V(D)J recombination (32). However, this is an unlikely explanation for the developmental block observed in tBrg1$^{-/-}$ thymocytes because TCR-β recombination and expression are unaffected by the loss of *Brg1* function (Fig. 6; reference 33). Interestingly, a similar block beyond the DN3 stage has been found in mice mutant for N-CoR, a chromatin-modifying complex that has been shown to contain Brg1, suggesting that the coordinated effort of multiple chromatin-modifying complexes are required for transition to the DP stage (34). The loss of the Brg1–N-CoR complex function is unlikely to fully explain the tBrg1$^{-/-}$ phenotype, however, because injection of anti-CD3ε, an antibody that mimics pre-TCR signaling, promotes DN→DP transition in N-CoR$^{-/-}$ thymocytes whereas in SWI–SNF-related mutant thymocytes it does not (33, 34). This result implicates the Brg1-containing complex(s) in mediating events downstream of the pre-TCR complex.

Signals emanating from the pre-TCR induce the cell proliferation and differentiation required for transition to the DP stage, raising the possibility that *Brg1* is required for regulation of genes essential for these processes. Indeed, BrdU incorporation in tBrg1$^{-/-}$ thymocytes revealed increased cell proliferation at the DN stages, indicating a cell cycle defect. Interestingly, Brg1 has been shown to interact with the retinoblastoma (*Rb*) and cyclin E gene products, both of which are required for the G1/S phase transition (35). Based on these data, it has been suggested that *Brg1* is a critical regulator of cell cycle progression and tumor suppression. This notion is consistent with an increase in total TN thymocytes in mutants, however, the severe reduction in total thymocytes, owing to an almost complete loss of DP cells, suggests a mechanism of active cell elimination before the DP stage. Indeed, using CD4 derepression to mark mutant cells, we observed increased apoptotic rates in DN populations, suggesting a coupling of cell proliferation to programmed cell death. In addition to the well-established role of *Rb* loss in tumor progression, a similar coupling of proliferation to apoptosis (p53-mediated) has been associated with *Rb* deficiency in a variety of cell types in animal models (35). In support of a similar Rb/E2F/p53 pathway operating in the thymic development, disruption of E2F1 leads to suppression of apoptosis and results in excess mature T cells (36). Moreover, p53 deficiency rescues the block in pre–T cell differentiation associated with CD3γ mutation (37). Therefore, given the interaction between *Brg1* and *Rb* pathway, loss of *Brg1* leading to aberrant Rb function, increased E2F-mediated transcription, and induction of p53-mediated apoptotic pathways provide a plausible explanation for the defects in thymocyte development in tBrg1$^{-/-}$ mice. However, we cannot rule out a role for *Brg1* in the cell survival–independent differentiation program underlying transition to the DP stage.

Due to the high efficiency of Cre-mediated recombination at the DN4 stage in +/floxed; *lck-Cre* mice and the severity of developmental block (low numbers of DP cells) in the thymus of tBrg1$^{-/-}$ mice, an unexpected result of our study was the presence of mature T cells in the periphery of these mutants. These T cell populations were shown to be a mixture of mutant and heterozygous (unrecombined floxed) cells, ruling out defective Cre-mediated recombination as the sole explanation for survival of these T lymphocytes. A parsimonious explanation for the survival of mutant cells is that in a small percentage of thymocytes, Cre-mediated recombination occurs relatively late in the DN4 stage and protein stability allows for clearing of key checkpoints required for further maturation. The mere existence of mature mutant T cells indicates that in contrast to developing thymocytes, *Brg1* is not required for survival of this more differentiated cell type. One could argue that because the *Brg1* mutation induced cell death at a highly proliferative stage of thymocyte development (β selection), perhaps *Brg1* would not be expected for survival in the more quiescent circulating mature T cell. Arguing against this view, however, is evidence for homeostatic proliferation occurring in the lymphopenic environment of tBrg1$^{-/-}$ mice. Interestingly, homeostatic proliferation of the limited number of surviving cells did not fully reconstitute peripheral T cell populations, contrary to the notion that a single T cell clone stimulated to generate memory T cells can fill the activated peripheral T cell pool (24, 38). Our results are consistent with more recent reports showing that limited numbers of naive T cells cannot fully reconstitute the periphery (39), indicating that loss of *Brg1* in these cells might not affect homeostasis, per se. The loss of Brg1 function did not, however, lead to deregulated cell proliferation and T cell–derived tumor formation in mutant animals aged over 18 mo, which stands in contrast to the high incidence of CD8$^+$ lymphomas observed through conditional inactivation of *SNF5*, another SWI–SNF-related complex member (40). Importantly, this finding supports the notion that the putative tumor suppressor function associated with *Brg1* loss of function mutations in neoplasms of humans and mice is tissue and cell type dependent and further, does not predispose cells of the mature T cell lineage to oncogenic transformation. Thus, taken together these results suggest that *Brg1* has inherently different functions with respect to cell survival and proliferation at different stages of T cell lineage specification.

We thank Daniel Metzger and Pierre Chambon for the *Brg1* floxed allele, Yuan Zhuang for the *lck-Cre* mice, and Gail Martin for the *Zp3-Cre* mice. We are also grateful to members of the Magnuson and Su labs for useful discussions and advice.

This work was supported by grants from the National Institutes of Health to T. Magnuson and L. Su.

Submitted: 1 May 2003
Accepted: 4 November 2003

References

1. Kuo, C.T., and J.M. Leiden. 1999. Transcriptional regulation of T lymphocyte development and function. *Annu. Rev. Im-*

munol. 17:149–187.
2. Workman, J.L., and R.E. Kingston. 1998. Alteration of nucleosome structure as a mechanism of transcriptional regulation. *Annu. Rev. Biochem.* 67:545–579.
3. Narlikar, G.J., H.Y. Fan, and R.E. Kingston. 2002. Cooperation between complexes that regulate chromatin structure and transcription. *Cell.* 108:475–487.
4. Bultman, S., T. Gebuhr, D. Yee, C. La Mantia, J. Nicholson, A. Gilliam, F. Randazzo, D. Metzger, P. Chambon, G. Crabtree, et al. 2000. A Brg1 null mutation in the mouse reveals functional differences among mammalian SWI/SNF complexes. *Mol. Cell.* 6:1287–1295.
5. Klochendler-Yeivin, A., L. Fiette, J. Barra, C. Muchardt, C. Babinet, and M. Yaniv. 2000. The murine SNF5/INI1 chromatin remodeling factor is essential for embryonic development and tumor suppression. *EMBO Rep.* 1:500–506.
6. Roberts, C.W., S.A. Galusha, M.E. McMenamin, C.D. Fletcher, and S.H. Orkin. 2000. Haploinsufficiency of Snf5 (integrase interactor 1) predisposes to malignant rhabdoid tumors in mice. *Proc. Natl. Acad. Sci. USA.* 97:13796–13800.
7. Kim, J.K., S.O. Huh, H. Choi, K.S. Lee, D. Shin, C. Lee, J.S. Nam, H. Kim, H. Chung, H.W. Lee, et al. 2001. Srg3, a mouse homolog of yeast SWI3, is essential for early embryogenesis and involved in brain development. *Mol. Cell. Biol.* 21:7787–7795.
8. Smale, S.T., and A.G. Fisher. 2002. Chromatin structure and gene regulation in the immune system. *Annu. Rev. Immunol.* 20:427–462.
9. Georgopoulos, K. 2002. Haematopoietic cell-fate decisions, chromatin regulation and ikaros. *Nat. Rev. Immunol.* 2:162–174.
10. Yeh, J.H., S. Spicuglia, S. Kumar, A. Sanchez-Sevilla, P. Ferrier, and J. Imbert. 2002. Control of IL-2Ralpha gene expression: structural changes within the proximal enhancer/core promoter during T-cell development. *Nucleic Acids Res.* 30:1944–1951.
11. Chi, T.H., M. Wan, K. Zhao, I. Taniuchi, L. Chen, D.R. Littman, and G.R. Crabtree. 2002. Reciprocal regulation of CD4/CD8 expression by SWI/SNF-like BAF complexes. *Nature.* 418:195–199.
12. Zhao, K., W. Wang, O.J. Rando, Y. Xue, K. Swiderek, A. Kuo, and G.R. Crabtree. 1998. Rapid and phosphoinositol-dependent binding of the SWI/SNF-like BAF complex to chromatin after T lymphocyte receptor signaling. *Cell.* 95: 625–636.
13. Geiman, T.M., and K. Muegge. 2000. Lsh, an SNF2/helicase family member, is required for proliferation of mature T lymphocytes. *Proc. Natl. Acad. Sci. USA.* 97:4772–4777.
14. Pan, L., J. Hanrahan, J. Li, L.P. Hale, and Y. Zhuang. 2002. An analysis of T cell intrinsic roles of E2A by conditional gene disruption in the thymus. *J. Immunol.* 168:3923–3932.
15. Lewandoski, M., K.M. Wassarman, and G.R. Martin. 1997. Zp3-cre, a transgenic mouse line for the activation or inactivation of loxP-flanked target genes specifically in the female germ line. *Curr. Biol.* 7:148–151.
16. Sumi-Ichinose, C., H. Ichinose, D. Metzger, and P. Chambon. 1997. SNF2beta-BRG1 is essential for the viability of F9 murine embryonal carcinoma cells. *Mol. Cell. Biol.* 17: 5976–5986.
17. Wakabayashi, Y., H. Watanabe, J. Inoue, N. Takeda, J. Sakata, Y. Mishima, J. Hitomi, T. Yamamoto, M. Utsuyama, O. Niwa, et al. 2003. Bcl11b is required for differentiation and survival of alphabeta T lymphocytes. *Nat. Immunol.* 4:533–539.
18. Nutt, S.L., B. Heavey, A.G. Rolink, and M. Busslinger. 1999. Commitment to the B-lymphoid lineage depends on the transcription factor Pax5. *Nature.* 401:556–562.
19. Lucas, B., F. Vasseur, and C. Penit. 1994. Production, selection, and maturation of thymocytes with high surface density of TCR. *J. Immunol.* 153:53–62.
20. Kovalev, G.I., D.S. Franklin, V.M. Coffield, Y. Xiong, and L. Su. 2001. An important role of CDK inhibitor p18(INK4c) in modulating antigen receptor-mediated T cell proliferation. *J. Immunol.* 167:3285–3292.
21. Vermes, I., C. Haanen, H. Steffens-Nakken, and C. Reutelingsperger. 1995. A novel assay for apoptosis. Flow cytometric detection of phosphatidylserine expression on early apoptotic cells using fluorescein labelled Annexin V. *J. Immunol. Methods.* 184:39–51.
22. Reisman, D.N., M.W. Strobeck, B.L. Betz, J. Sciariotta, W. Funkhouser, Jr., C. Murchardt, M. Yaniv, L.S. Sherman, E.S. Knudsen, and B.E. Weissman. 2002. Concomitant down-regulation of BRM and BRG1 in human tumor cell lines: differential effects on RB-mediated growth arrest vs CD44 expression. *Oncogene.* 21:1196–1207.
23. Fischer, A., and B. Malissen. 1998. Natural and engineered disorders of lymphocyte development. *Science.* 280:237–243.
24. Freitas, A.A., and B. Rocha. 2000. Population biology of lymphocytes: the flight for survival. *Annu. Rev. Immunol.* 18: 83–111.
25. Shimizu, C., H. Kawamoto, M. Yamashita, M. Kimura, E. Kondou, Y. Kaneko, S. Okada, T. Tokuhisa, M. Yokoyama, M. Taniguchi, et al. 2001. Progression of T cell lineage restriction in the earliest subpopulation of murine adult thymus visualized by the expression of lck proximal promoter activity. *Int. Immunol.* 13:105–117.
26. Valitutti, S., S. Muller, M. Dessing, and A. Lanzavecchia. 1996. Different responses are elicited in cytotoxic T lymphocytes by different levels of T cell receptor occupancy. *J. Exp. Med.* 183:1917–1921.
27. Tough, D.F., and J. Sprent. 1994. Turnover of naive- and memory-phenotype T cells. *J. Exp. Med.* 179:1127–1135.
28. Jameson, S.C. 2002. Maintaining the norm: T-cell homeostasis. *Nat. Rev. Immunol.* 2:547–556.
29. Ward, J.M., M.R. Anver, D.C. Haines, J.M. Melhorn, P. Gorelick, L. Yan, and J.G. Fox. 1996. Inflammatory large bowel disease in immunodeficient mice naturally infected with *Helicobacter hepaticus*. *Lab. Anim. Sci.* 46:15–20.
30. Shomer, N.H., C.A. Dangler, M.D. Schrenzel, and J.G. Fox. 1997. *Helicobacter bilis*-induced inflammatory bowel disease in scid mice with defined flora. *Infect. Immun.* 65:4858–4864.
31. Li, X., J.G. Fox, M.T. Whary, L. Yan, B. Shames, and Z. Zhao. 1998. SCID/NCr mice naturally infected with *Helicobacter hepaticus* develop progressive hepatitis, proliferative typhlitis, and colitis. *Infect. Immun.* 66:5477–5484.
32. Kwon, J., K.B. Morshead, J.R. Guyon, R.E. Kingston, and M.A. Oettinger. 2000. Histone acetylation and hSWI/SNF remodeling act in concert to stimulate V(D)J cleavage of nucleosomal DNA. *Mol. Cell.* 6:1037–1048.
33. Chi, T.H., M. Wan, P.P. Lee, K. Akashi, D. Metzger, P. Chambon, C.B. Wilson, and G.R. Crabtree. 2003. Sequential roles of Brg, the ATPase subunit of BAF chromatin remodeling complexes, in thymocyte development. *Immunity.* 19:169–182.
34. Jepsen, K., O. Hermanson, T.M. Onami, A.S. Gleiberman, V. Lunyak, R.J. McEvilly, R. Kurokawa, V. Kumar, F. Liu,

E. Seto, et al. 2000. Combinatorial roles of the nuclear receptor corepressor in transcription and development. *Cell.* 102: 753–763.

35. Zhang, H.S., M. Gavin, A. Dahiya, A.A. Postigo, D. Ma, R.X. Luo, J.W. Harbour, and D.C. Dean. 2000. Exit from G1 and S phase of the cell cycle is regulated by repressor complexes containing HDAC-Rb-hSWI/SNF and Rb-hSWI/SNF. *Cell.* 101:79–89.
36. Field, S.J., F.Y. Tsai, F. Kuo, A.M. Zubiaga, W.G. Kaelin, Jr., D.M. Livingston, S.H. Orkin, and M.E. Greenberg. 1996. E2F-1 functions in mice to promote apoptosis and suppress proliferation. *Cell.* 85:549–561.
37. Haks, M.C., P. Krimpenfort, J.H. van den Brakel, and A.M. Kruisbeek. 1999. Pre-TCR signaling and inactivation of p53 induces crucial cell survival pathways in pre-T cells. *Immunity.* 11:91–101.
38. Tanchot, C., and B. Rocha. 1997. Peripheral selection of T cell repertoires: the role of continuous thymus output. *J. Exp. Med.* 186:1099–1106.
39. Tanchot, C., A. Le Campion, B. Martin, S. Leaument, N. Dautigny, and B. Lucas. 2002. Conversion of naive T cells to a memory-like phenotype in lymphopenic hosts is not related to a homeostatic mechanism that fills the peripheral naive T cell pool. *J. Immunol.* 168:5042–5046.
40. Roberts, C.W., M.M. Leroux, M.D. Fleming, and S.H. Orkin. 2002. Highly penetrant, rapid tumorigenesis through conditional inversion of the tumor suppressor gene Snf5. *Cancer Cell.* 2:415–425.